

High Performance Blue Phase Liquid Crystals Stabilized by Linear Photopolymers

Daming Xu*, Jiamin Yuan*, Martin Schadt**, Shin-Tson Wu*

*College of Optics and Photonics, University of Central Florida, Orlando FL 32816, USA

** MS High-Tech Consulting, Liestalerstrasse 77, 4411 Seltisberg, Switzerland

Abstract

We experimentally demonstrated an in-plane switching (IPS) BPLC stabilized by linear photo-polymerization (LPP) for the first time. The LPP-process helps reduce response time by 2X and suppress hysteresis from 6.95% to 0.36%. It plays an important role to guide future BPLC material and device development as well as manufacturing process.

Author Keywords

Blue phase; liquid crystal; electrostriction; linear photopolymer.

1. Introduction

Polymer-stabilized blue phase liquid crystal (PS-BPLC) [1] is emerging as a strong candidate for next-generation display [2-4] and photonic applications [5-7]. Compared to nematic liquid crystals [8-11], PS-BPLCs exhibit some attractive features: submillisecond gray-to-gray response time, no need for surface alignment, optically isotropic dark state, etc. After a decade of extensive efforts, major technical challenges of PS-BPLCs have been resolved. By implementing large Kerr constant BPLC materials [12-14] and using device structures with enhanced penetrating fields [15-17], the operation voltage has been reduced from 50V to below 10V. Meanwhile, high transmittance (>80%) can be achieved through optimizing the refraction effect of the non-uniform electric fields [18]. Moreover, an over 3000:1 contrast ratio has been demonstrated by compensating the polarization rotation effect of PS-BPLC cells [19, 20].

In terms of the device configuration, both in-plane-switching (IPS) [15-17] and vertical field switching [21, 22] modes have been developed. Between these two, IPS is more commonly employed because of its simpler backlight system and fabrication. However, for IPS cells, hysteresis and prolonged response times, especially in the high field region, remain as technical challenges [23, 24]. From previous studies [25, 26], three electric field-induced effects occur in a PS-BPLC as the electric field increases: local LC director reorientation governed by Kerr effect, lattice distortion induced by electrostriction, and finally transition into a LC phase with lower symmetry. The latter two processes are major reasons causing hysteresis and slow response time. Therefore, there is an urgent need to suppress the electrostriction and phase transition effects in order to achieve fast-response and hysteresis-free BPLC devices.

In this paper, we experimentally demonstrate an IPS BPLC stabilized by linear photo-polymerization (LPP) for the first time. Compared to conventional unpolarized-UV curing, the LPP-stabilized IPS BPLC shows 2X faster response time and reduces hysteresis from 6.95% to 0.36%.

2. Experiment

To form polymer network for stabilizing the BPLC lattice, two types of monomers are commonly used: a di-functional (e.g. RM257) monomer is mixed with a mono-functional [e.g. dodecyl acrylate (C12A)] or a tri-functional monomer [e.g. 1,1,1-trimethylolpropane triacrylate (TMPTA)]. The chemical structures of these exemplary monomers are depicted in Fig. 1.

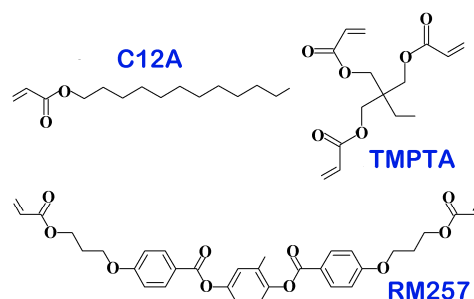


Figure 1. Chemical structures of monomers employed in our PS-BPLC.

In the past, the polymerization process of pre-polymers in PS-BPLC was commonly conducted by using unpolarized UV light. However, the photo-crosslinking mechanism of pre-polymers is polarization-dependent [27, 28]. Hence, by crosslinking double bonds with a linearly polarized UV light, anisotropic polymer networks can be formed. By controlling the UV polarization axis with respect to the direction of the stripe electrodes of an IPS-BPLC cell, the formed anisotropic polymer network could result in anisotropic electrostriction correspondingly.

In our experiments, we employed a large $\Delta\epsilon$ nematic LC host JC-BP07N (JNC, Japan) whose physical properties are: $\Delta n = 0.162$ at $\lambda = 633$ nm, $\Delta\epsilon = 302$ at 100 Hz and 22°C, and $T_c = 87^\circ\text{C}$. The BPLC precursor consists of 86.53 wt.% JC-BP07N, 2.82 wt.% chiral dopant R5011 (HCCH), 6.31 wt.% RM257 (Merck), 4.02 wt.% C12A (Sigma Aldrich) and 0.32 wt.% photoinitiator. The BPLC precursor was heated to an isotropic phase and then filled into IPS cells (cell gap $d \sim 7.3$ μm , electrode width $w = 8$ μm , spacing $l = 12$ μm) without polyimide alignment layer.

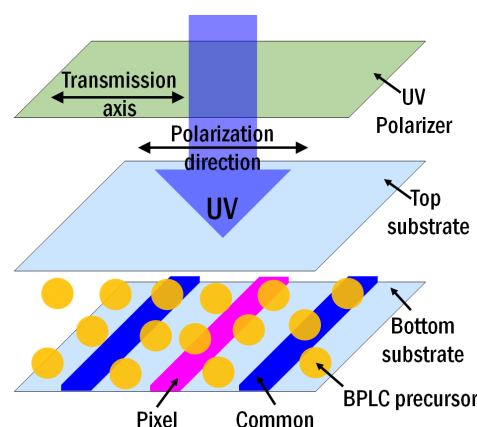


Figure 2. Experimental setup of curing process of LPP-stabilized BPLC cell.

To investigate the effect of UV polarization on the electro-optic properties of BPLCs, we first prepared three IPS samples exposed under different UV polarization conditions. The directions of UV polarization

were parallel and perpendicular to the stripe electrodes in Sample 1 and 2, respectively; whereas Sample 3 was cured by unpolarized UV light. To rule out possible disturbing influences due to temperature cooling rate and curing temperature [29] we kept these two parameters identical for all three samples. A linear UV polarizer is placed between UV light source and BPLC cell in all polarized-exposure experiments, as shown in Fig. 2. All the samples were illuminated with UV light for 15 min ($\lambda \sim 365$ nm, intensity 8 mW/cm^2).

3. Results and discussion

(a) Effect of UV Polarization: To evaluate the degree of electrostriction, we measured the hysteresis of each sample, as depicted in Fig. 3. Their operation voltage, hysteresis, and response time are listed in Table 1. From the table we find that Sample 2 exhibits a much smaller hysteresis than Sample 3 (unpolarized light). The physical mechanism is explained as follows. In the BPLC precursor containing C12A and RM257 monomers, the directional LPP photoreaction is parallel to the polarization axis of the incident linearly polarized UV radiation. As a result, the polymer network is stronger along the UV polarization axis [27], i.e. parallel to the direction of the applied electric field in Sample 2, as illustrated in Fig. 4(b). Therefore, the polymer network in Sample 2 is more robust against electric field-induced deformation or distortion along the LPP direction [30], leading to a suppressed electrostriction effect and a reduced hysteresis. However, for UV polarization parallel to the stripe electrodes (Sample 1), the polymer network forms mainly along the electrode direction and is therefore less robust along the direction of the applied electric field, (c.f. Fig. 4(a)). Consequently, the polymer network is more likely to be distorted or deformed by the applied electric field in the configuration of Fig. 4(a), resulting in severe electrostriction. This is indeed observed in Sample 1, which exhibits the largest hysteresis (7.56%) as depicted in Fig. 3.

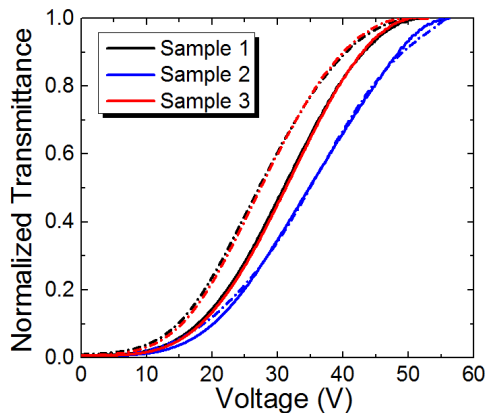


Figure 3. Hysteresis loops of Samples 1-3 (Solid lines: forward driving, dashed lines: backward driving).

TABLE I. Measured operation voltage, hysteresis, response time, fitted time constants and contribution of electrostriction effect of Samples 1-3.

	Sample 1	Sample 2	Sample 3
V_{on} (V)	51.8	56.2	53.0
Hysteresis	7.56%	0.36%	6.95%
τ_{rise} (μs)	674.6	456.8	524.7
τ_{decay} (ms)	4.34	1.90	3.72
t_1 (ms)	0.51	0.27	0.39
t_2 (ms)	6.47	3.78	5.98
$A_2/(A_1 + A_2)$	43.8%	16.9%	38.7%

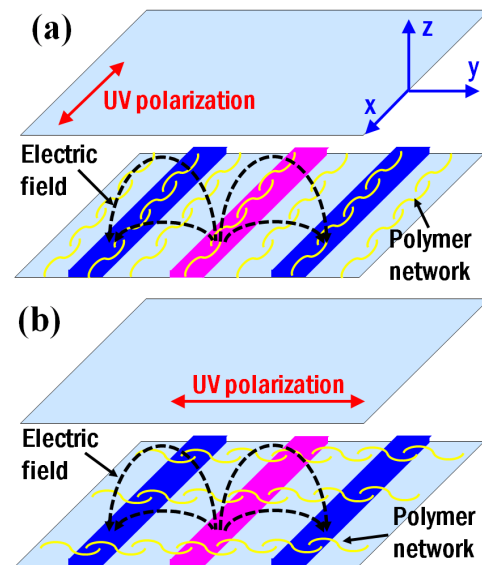


Figure 4. LPP-induced anisotropic polymer network in (a) Sample 1 and (b) Sample 2.

As listed in Table 1, Sample 2 exhibits the fastest rise and decay times while Sample 1 is the slowest. To explain the difference, we used a double relaxation model [31] to reveal the contributions of Kerr and electrostriction effects. Each cell was driven to peak transmittance after which the voltage was instantaneously removed and the transient transmittance change was recorded by an oscilloscope. The measured change in transmittance T is related to the phase retardation ϕ by:

$$T = \sin^2(\phi / 2). \quad (1)$$

Then we fit measured data with following double relaxation equation:

$$\phi(t) = A_1 e^{-t/t_1} + A_2 e^{-t/t_2}, \quad (2)$$

where t_1 and t_2 are the average decay time constants and A_1 and A_2 are the phase retardations due to Kerr effect and electrostriction, respectively. The double exponential equation is commonly used to characterize a two mechanism-involved dynamic process [32].

The fitted time constants and the contribution of electrostriction effect, which is denoted by $A_2/(A_1 + A_2)$, are also included in Table 1. All the values of t_1 lie in the submillisecond range while those of t_2 are several milliseconds, well matches with the fast Kerr effect and the slow electrostriction effect. Please note that Sample 2 exhibits the fastest response time. This is due to the suppression of electrostriction by polarized crosslinking, which can be seen from the smallest $A_2/(A_1 + A_2)$ ratio of Sample 2. However, from Fig. 4 the non-planar electric field at the edges of planar stripe electrodes is still quite strong, therefore the electrostriction effect is still not negligible (16.9%). Nevertheless, compared to Sample 3 which is stabilized by unpolarized UV light, this ratio is more than 2X smaller. By using protruded or etched electrodes instead of planar electrodes, the on-state voltage would drop to $<10\text{V}$, which will be outlined later, and the electrostriction effect should be completely suppressed. As a result, the response time should be in the submillisecond range over the entire driving voltage range.

(b) Effect of UV Intensity: Meanwhile, the illumination intensity of polarized UV light affects the rate and the anisotropy of the crosslinking process. In addition to Sample 2, we prepared two more samples using different UV exposure intensities for comparison. The UV dosage for all three samples was the same: 8 mW/cm^2 for 15 min, 4 mW/cm^2 for 30 min, and 2 mW/cm^2 for 60 min. The measured hysteresis loops of these three samples are plotted in Fig. 5 and the

numerical values of their operation voltages, hysteresis, and response times are listed in Table 2. With increasing UV exposure intensity, electrostriction is suppressed, resulting in faster response time and reduced hysteresis. This trend is similar to the LPP process of azo-type monomers, in which the diffusion rate of linearly polarized pre-polymers is proportional to the illumination power according to the diffusion model of photopolymers [33]. Hence, here we use this model as an analogy to explain the correlation of UV intensity and LPP-induced anisotropy in PS-BPLC. The higher diffusion rate under stronger UV illumination power is expected to result in a larger anisotropy of polymer networks. Consequently, a stronger polymer network forms along the electric field direction, thus suppressing electrostriction. In analogy, lower UV illumination power reduces the anisotropy of polymer networks. Hence, to induce a large anisotropy in the polymer networks of PS-BPLCs for minimizing electrostriction, strong linearly polarized UV light is preferred.

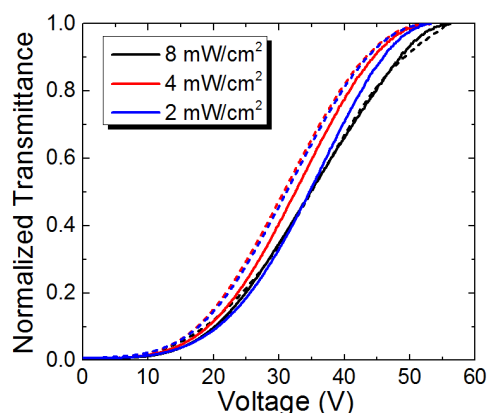


Figure 5. Hysteresis loops of IPS cells under different UV illumination intensities (Solid lines: forward driving, dashed lines: backward driving).

TABLE 2. Measured operation voltage, hysteresis and response time of IPS cells under different UV intensities.

	2 mW/cm ²	4 mW/cm ²	8 mW/cm ²
V_{on} (V)	53.2	54.0	56.2
Hysteresis	6.79%	3.40%	0.36%
τ_{rise} (μ s)	860.5	594.5	456.8
τ_{decay} (ms)	3.67	2.78	1.90

(c) Monomer selection: Besides the monomer combination of RM257 and C12A discussed above, we also investigated the effect of LPP on the electro-optic properties of PS-BPLCs by using another monomer combination, namely the di-functional monomer RM257 and the tri-functional monomer TMPTA. The blue phase precursor consists of 86.90 wt. % JC-BP07N, 2.81 wt. % chiral dopant R5011, 5.98 wt. % RM257, 3.99 wt. % TMPTA and 0.32 wt. % photoinitiator. This time, we also prepared three IPS samples under different UV curing conditions. The directions of UV polarization were parallel and perpendicular to the stripe electrodes in Sample 4 and 5, respectively; whereas Sample 6 was illuminated by unpolarized UV light. All three samples were polymerized with the same UV dosage with: 8 mW/cm² for 15 minutes.

The measured hysteresis loops of these three samples are plotted in Fig. 6, and the numerical values of their operation voltage, hysteresis as well as response time are listed in Table 3. Compared to the combination of RM257 and C12A, the samples comprising RM257 and TMPTA exhibit much faster response time. This results from the fact that the tri-

functional monomer TMPTA has three photo-crosslinking double bonds, which can form much stronger polymer network than the mono-functional monomer C12A. Nevertheless, these three samples do not exhibit large differences in terms of operation voltage, hysteresis and response time under different UV polarization directions. This is because the three photo-crosslinking double bonds of TMPTA are along different directions, thus rendering their polymer networks more likely to be isotropic no matter which direction is the UV light polarized along. Therefore, in order to use of the LPP-stabilization for the purpose of suppressing electrostriction effect, the combination of monomer-functional and di-functional monomers should be chosen.

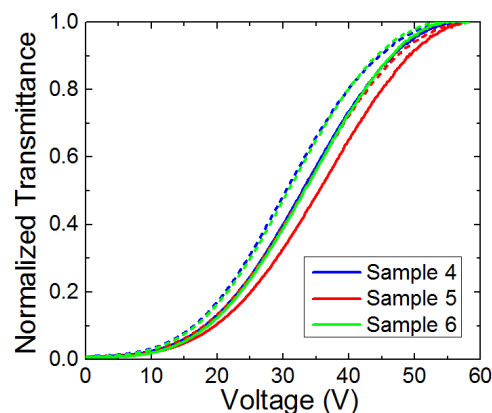


Figure 6. Measured hysteresis loops of Samples 4-6. (Solid lines: forward driving, dashed lines: backward driving).

TABLE 3. Measured operation voltage, hysteresis, and response time of Samples 4-6.

	Sample 4	Sample 5	Sample 6
V_{on} (V)	57.2	58.0	58.0 V
Hysteresis	4.37%	3.97%	4.14%
τ_{rise} (μ s)	362.9	369.3	345.8
τ_{decay} (μ s)	958.4	810.7	871.5

4. Conclusion

In conclusion, we propose a method to suppress the electrostriction in PS-BPLCs via polymerizing photopolymers with linearly polarized UV light. By illuminating the BPLC pre-polymers with linearly polarized UV light, anisotropic polymer networks are formed, resulting in anisotropic electrostriction. Linear polarization of the cross-linking UV light perpendicular to the stripe electrodes strongly suppresses electrostriction. The resulting hysteresis is reduced from 6.95% to 0.36% and the response times improve by a factor of two. To induce a larger anisotropy in the polymer network so that the electrostriction effect can be further reduced, a more powerful linearly polarized UV exposure is required. It is foreseeable that the LPP-stabilization method will become a guideline for future BPLC manufacturing process.

5. Acknowledgments

The authors are indebted to Dr. Yasuhiro Haseba of JNC for providing the JC-BP07N sample and Industrial Technology Research Institute (ITRI, Taiwan) for the financial support.

6. References

- [1] H. Kikuchi, M. Yokota, Y. Hisakado, H. Yang, T. Kajiyama, "Polymer-stabilized liquid crystal blue phases," *Nature Mater.* **1**, 64-68 (2002).
- [2] J. Yan, L. Rao, M. Jiao, Y. Li, H. C. Cheng, S. T. Wu, "Polymer-stabilized optically isotropic liquid crystals for next-generation display and photonics applications," *J. Mater. Chem.* **21**, 7870-7877 (2011).
- [3] Z. Luo, D. Xu, S. T. Wu, "Emerging quantum-dots-enhanced LCDs," *J. Disp. Technol.* **10**, 526-539 (2014).
- [4] G. Nordendorf, A. Hoischen, J. Schmidtke, D. Wilkes, H.-S. Kitzerow, "Polymer-stabilized blue phases: promising mesophases for a new generation of liquid crystal displays," *Polymer. Adv. Tech.* **25**, 1195-1207 (2014).
- [5] S. Yokoyama, S. Mashiko, H. Kikuchi, K. Uchida, T. Nagamura, "Laser emission from a polymer-stabilized liquid-crystalline blue phase," *Adv. Mater.* **18**, 48-51 (2006).
- [6] Y. H. Lin, H. S. Chen, H. C. Lin, Y. S. Tsou, H. K. Hsu, W. Y. Li, "Polarizer-free and fast response microlens arrays using polymer-stabilized blue phase liquid crystals," *Appl. Phys. Lett.* **96**, 113505 (2010).
- [7] H. Y. Liu, C. T. Wang, C. Y. Hsu, T. H. Lin, J. H. Liu, "Optically tunable blue phase photonic band gaps," *Appl. Phys. Lett.* **96**, 121103 (2010).
- [8] D. Xu, L. Rao, C. D. Tu, S. T. Wu, "Nematic liquid crystal display with submillisecond grayscale response time," *J. Disp. Technol.* **9**, 67-70 (2013).
- [9] M. Xu, D. Xu, H. Ren, I. S. Yoo, Q. H. Wang, "An adaptive liquid lens with radial interdigitated electrode," *J. Opt.* **16**, 105601 (2014).
- [10] H. Chen, F. Peng, Z. Luo, D. Xu, S. T. Wu, M. C. Li, S. L. Lee, W. C. Tsai, "High performance liquid crystal displays with a low dielectric constant material," *Opt. Mater. Express* **4**, 2262-2273 (2014).
- [11] D. Xu, H. Chen, S. T. Wu, M. C. Li, S. L. Lee, W. C. Tsai, "A fringe field switching liquid crystal display with fast grayscale response time," *J. Disp. Technol.* **11**, 353-359 (2015).
- [12] M. Wittek, N. Tanaka, D. Wilkes, M. Bremer, D. Pauluth, J. Canisius, A. Yeh, R. Yan, K. Skjonnemand, M. Klasen-Memmer, "New materials for polymer-stabilized blue phase," *SID Int. Symp. Digest Tech. Papers* **43**, 25-28 (2012).
- [13] Y. Haseba, S. Yamamoto, K. Sago, A. Takata, H. Tobata, "Low-voltage polymer-stabilized blue-phase liquid crystals," *SID Int. Symp. Digest Tech. Papers* **44**, 254-257 (2013).
- [14] Y. Chen, D. Xu, S. T. Wu, S. Yamamoto, Y. Haseba, "A low voltage and submillisecond-response polymer-stabilized blue phase liquid crystal," *Appl. Phys. Lett.* **102**, 141116 (2013).
- [15] L. Rao, Z. Ge, S. T. Wu, S. H. Lee, "Low voltage blue-phase liquid crystal displays," *Appl. Phys. Lett.* **95**, 231101 (2009).
- [16] L. Rao, H. C. Cheng, S. T. Wu, "Low voltage blue-phase LCDs with double-penetrating fringe fields," *J. Disp. Technol.* **6**, 287-289 (2010).
- [17] C. Y. Tsai, T. J. Tseng, L. Y. Wang, F. C. Yu, Y. F. Lan, P. J. Huang, S. Y. Lin, K. M. Chen, B. S. Tseng, C. W. Kuo, C. H. Lin, J. K. Lu, N. Sugiura, "Polymer-stabilized blue phase liquid crystal displays applying novel groove cell structure," *SID Int. Symp. Digest Tech. Papers* **44**, 182-183 (2013).
- [18] D. Xu, Y. Chen, Y. Liu, S. T. Wu, "Refraction effect in an in-plane-switching blue phase liquid crystal cell," *Opt. Express* **21**, 24721-24735 (2013).
- [19] Y. Liu, Y. F. Lan, H. X. Zhang, R. Zhu, D. Xu, C. Y. Tsai, J. K. Lu, N. Sugiura, Y. C. Lin, S. T. Wu, "Optical rotatory power of polymer-stabilized blue phase liquid crystals," *Appl. Phys. Lett.* **102**(2013).
- [20] Y. F. Lan, Y. Liu, P. J. Huang, D. Xu, C. Y. Tsai, C. H. Lin, N. Sugiura, S. T. Wu, "Non-ideal optical isotropy of blue phase liquid crystal," *Appl. Phys. Lett.* **105**, 011903 (2014).
- [21] H. C. Cheng, J. Yan, T. Ishinabe, S. T. Wu, "Vertical field switching for blue-phase liquid crystal devices," *Appl. Phys. Lett.* **98**, 261102 (2011).
- [22] J. Yan, D. Xu, H. C. Cheng, S. T. Wu, Y. F. Lan, C. Y. Tsai, "Turning film for widening the viewing angle of a blue phase liquid crystal display," *Appl. Opt.* **52**, 8840-8844 (2013).
- [23] K. M. Chen, S. Gauza, H. Q. Xianyu, S. T. Wu, "Submillisecond Gray-Level Response Time of a Polymer-Stabilized Blue-Phase Liquid Crystal," *J. Disp. Technol.* **6**, 49-51 (2010).
- [24] Y. Liu, S. Xu, D. Xu, J. Yan, Y. Gao, S. T. Wu, "A hysteresis-free polymer-stabilized blue-phase liquid crystal," *Liq. Cryst.* **41**, 1339-1344 (2014).
- [25] J. Kerr, "A new relation between electricity and light: Dielectric media birefringent," *Philos. Mag.* **50**, 337-348 (1875).
- [26] H. S. Kitzerow, P. P. Crooker, S. L. Kwok, J. Xu, G. Heppke, "Dynamics of blue-phase selective reflections in an electric-field," *Phys. Rev. A* **42**, 3442-3448 (1990).
- [27] M. Schadt, K. Schmitt, V. Kozinkov, V. Chigrinov, "Surface-induced parallel alignment of liquid-crystals by linearly polymerized photopolymers," *Jpn. J. Appl. Phys.* **31**, 2155-2164 (1992).
- [28] M. Schadt, H. Seiberle, A. Schuster, "Optical patterning of multidomain liquid-crystal displays with wide viewing angles," *Nature* **381**, 212-215 (1996).
- [29] C. Y. Fan, H. C. Jau, T. H. Lin, F. C. Yu, T. H. Huang, C. Y. Liu, N. Sugiura, "Influence of polymerization temperature on hysteresis and residual birefringence of polymer stabilized blue phase LCs," *J. Disp. Technol.* **7**, 615-618 (2011).
- [30] D. Xu, J. Yuan, M. Schadt, S. T. Wu, "Blue phase liquid crystals stabilized by linear photo-polymerization," *Appl. Phys. Lett.* **105**, 081114 (2014).
- [31] D. Xu, J. Yan, J. Yuan, F. Peng, Y. Chen, S. T. Wu, "Electro-optic response of polymer-stabilized blue phase liquid crystals," *Appl. Phys. Lett.* **105**, 011119 (2014).
- [32] D. Xu, F. Peng, H. Chen, J. Yuan, S. T. Wu, M. C. Li, S. L. Lee, W. C. Tsai, "Image sticking in liquid crystal displays with lateral electric fields," *J. Appl. Phys.* **116**, 193102 (2014).
- [33] V. Chigrinov, S. Pikin, A. Verevochnikov, V. Kozenkov, M. Khazimullin, J. Ho, D. D. Huang, H. S. Kwok, "Diffusion model of photoaligning in azo-dye layers," *Phys. Rev. E* **69**, 061713 (2004).